Effects of single and combined exposures of gold (nano *versus* ionic form) and gemfibrozil in a liver organ culture of *Sparus aurata*

A. Barreto[1*], A. Carvalho[1], D. Silva[1], E. Pinto[2], A. Almeida[3], P. Paíga[4], L. Correira-Sá[4], C. Delerue-Matos[4], T. Trindade[5], A.M.V.M. Soares[1], K. Hylland[6], S. Loureiro[1], M. Oliveira[1]

[1] Departamento de Biologia & CESAM, Universidade de Aveiro, 3810-193 Aveiro, Portugal

[2] LAQV/REQUIMTE, Departamento de Ciências Químicas, Faculdade de Farmácia, Universidade do Porto, Rua Jorge Viterbo Ferreira, 228, 4050-313 Porto, Portugal & Departamento de Saúde Ambiental, Escola Superior de Saúde, P. Porto. CISA/Centro de Investigação em saúde e Ambiente, Rua Dr. António Bernardino de Almeida, 400. 4200-072 Porto, Portugal

[3] LAQV/REQUIMTE, Departamento de Ciências Químicas, Faculdade de Farmácia, Universidade do Porto, Rua Jorge Viterbo Ferreira, 228, 4050-313 Porto, Portugal

[4] REQUIMTE/LAQV, Instituto Superior de Engenharia do Porto, Instituto Politécnico do Porto, Rua Dr. António Bernardino de Almeida, 431, 4200-072 Porto, Portugal

[5] Departamento de Química & CICECO - Aveiro Instituto de Materiais, Universidade de Aveiro, 3810-193 Aveiro, Portugal

[6] Department of Biosciences, University of Oslo, PO Box 1066, N-0316 Oslo, Norway

*Corresponding author: E-mail: abarreto@ua.pt, Tel +351 234 370 350, Fax +351 234 372 587

Highlights

- *In vitro*, gold nanoparticles (AuNPs) damaged fish liver DNA and cellular membranes;
- Gemfibrozil (GEM) caused DNA damage at 1.5 µg.L^{-1};

- Overall, effects of AuNPs+GEM were higher than predicted, based on single exposures;
- Liver organ culture proved sensitive and a valuable *in vitro* model.

Abstract

In vitro methods have gained increasing importance in ecotoxicology due to ethical concerns. The aim of this study was to assess the *in vitro* effects of gold, in the nanoparticle (AuNPs) and ionic (Au^{+}) form, and the pharmaceutical gemfibrozil (GEM), in single and combined exposures. Fish liver was 24 h exposed to gold (4 to 7,200 $\mu g.L^{-1}$), GEM (1.5 to 15,000 $\mu g.L^{-1}$) and combination 80 $\mu g.L^{-1}$ gold + 150 $\mu g.L^{-1}$ GEM. Endpoints related with antioxidant status, peroxidative and genetic damage were assessed. AuNPs caused more effects than Au^{+}, increasing catalase and glutathione reductase activities and damaging DNA and cellular membranes. Effects were dependent on AuNPs size, coating and concentration. GEM damaged DNA at an environmentally relevant concentration, 1.5 $\mu g.L^{-1}$. Overall, the effects of the combined exposures were higher than the predicted, based on single exposures. This study showed that liver culture can be a useful model to study contaminants effects.

Keywords: Fish liver culture; gilthead seabream; nanotoxicology; ionic gold; oxidative stress; DNA integrity.

1. Introduction

Due to concerns regarding animal welfare, time and cost constraints, and generation of dangerous residues, establishing workable *in vitro* systems became a priority. In this perspective, the use of organ/cell cultures has the advantage of allowing a reduction in the number of animals used per test, improved control of environmental conditions, reduction of the genetic heterogeneity and chemicals needed, as well as a reduction in waste (Oliveira et al. 2003; Soldatow et al 2013). Liver cell culture models can be important in toxicological research due to the crucial function of this organ in detoxification, metabolic and inflammatory/immune processes (Zeilinger et al. 2016). Although liver cell cultures, including the ones obtained from fish (Franco et al. 2019), are well-established biological methodologies in *in vitro* testing, organ cultures allow the study of effects in a more physiologically relevant context. The use of liver slices retain the 3D structure, contain all liver cell types and show good *in vitro*/*in vivo* correlation for xenobiotic metabolism (Soldatow et al 2013). Despite the successful use of animals organ cultures in toxicological research, fish organ cultures have not been extensively used in ecotoxicology, despite the reported value to assess the effects of chromium in *Anguilla anguilla* (Oliveira et al. 2003) and to test different oxytetracycline exposure methods, using *Danio rerio* (Chemello et al. 2019).

The effects of gold nanoparticles (AuNPs) and the lipid regulator gemfibrozil (GEM) on marine fish remains largely unknown despite their increasing production, use and disposal. Previous *in vivo* studies with gilthead seabream (*Sparus aurata*) have already shown the ability of AuNPs (e.g., Barreto et al. 2020) and GEM (e.g., Barreto et al. 2017, 2018) to induce toxic effect alone and in combined exposures

(Barreto et al. 2019a, 2019b). Considering the reported importance of the liver in AuNPs accumulation (Chen et al. 2013; Iswarya et al. 2016; Khan, Vishakante, and Siddaramaiah 2013; Mateo et al. 2014; Simpson et al. 2013) and metabolization of xenobiotics allied with the need to use methodologies that minimize the need to sacrifice animals providing reliable information in terms of effects and mechanisms of action of emerging contaminants, this study aimed to assess the effects of AuNPs and GEM, alone and in combined exposures, in liver cultures. Effects after 24 h exposure were evaluated measuring endpoints related with oxidative stress, peroxidative and DNA damage.

2. Material and Methods

2.1. Test organisms

Juvenile gilthead seabream (*Sparus aurata*), length 100 ± 0.4 cm, acquired from a Spanish aquaculture facility (Santander, Spain). Fish were acclimated for 4 weeks in 250 L aquaria, at a ratio bellow 1 g of fish per 1 L of aerated and filtered (Eheim filters) artificial seawater (ASW; Ocean Fish, Prodac), prepared by dissolving the salt in reverse osmosis purified water to obtain a salinity of 30. Fish were maintained in a room-controlled temperature (20 ºC) with natural photoperiod. During this period, animals were fed daily with commercial fish food (Sorgal, Portugal) at a ratio of 1% of body weight/day. All experimental procedures followed International Guiding Principles for Biomedical Research Involving Animals (EU 2010/63) and were previously approved by the ethics committee and the responsible national legal authority “Direção Geral de Alimentação e Veterinária” (authorization N421/2013).

2.2. Synthesis and characterisation of gold nanoparticles (AuNPs)

Citrate-coated AuNPs (cAuNPs), diameter of 7 nm, were synthesised using the pH-shifting method, with reduction of gold (III) chloride trihydrate by citric acid, followed by neutralization with NaOH (Shiba 2013). cAuNPs, diameter of 40 nm, were prepared, using 15 nm seeds, by sodium citrate reduction of gold (III) chloride trihydrate (Lekeufack et al. 2010). Part of cAuNPs were coated with PVP as described by Barreto et al. (2015). Both coated AuNPs – cAuNPs and PVP coated AuNPs (PVP-AuNPs) – were centrifuged and the pellet resuspended in ultrapure water. AuNPs were characterised in ultrapure water and in the media used for the experiments – Dulbecco's Modified Eagle's medium with fetal bovine serum (DMEM+FBS) – by UV-Vis spectrophotometry (Cintra 303, GBC Scientific) to obtain the UV-Vis spectra; hydrodynamic size was assessed by dynamic light scattering – DLS (Zetasizer Nano ZS, Malvern) and size/shape evaluated by transmission electron microscopy – TEM (Hitachi, H9000 NAR) or scanning electron microscopy – SEM (Hitachi, SU70). Zeta potential (ZP) was measured using Zetasizer (Nano ZS, Malvern). Measurements were performed at 0, 12 and 24 h, at concentrations higher than 80 $\mu g.L^{-1}$, considering that, for concentrations lower than 80 $\mu g.L^{-1}$ the detection limits of the used techniques did not allow the characterisation of AuNPs. The characterisation was also performed visually, assessing the colour of the AuNPs suspensions.

2.3. Liver organ culture exposures

DMEM+FBS was prepared as follow: 50% DMEM, 40% ultrapure water, 1 mM of glutamine, 15 mM HEPES, 10% FBS and 100 $\mu g.mL^{-1}$ antibiotics (penicillin and

122 streptomycin). A stock solution of GEM (50 $g.L^{-1}$) was prepared in dimethyl sulfoxide
123 (DMSO) and test solutions prepared by the dilution of the stock in DMEM+FBS. Test
124 suspensions of AuNPs were prepared in DMEM+FBS from cAuNPs (100 and 97
125 $mg.L^{-1}$ for 7 and 40 nm, respectively) and PVP-AuNPs (78 and 58 $mg.L^{-1}$ for 7 and
126 40 nm, respectively) stock suspensions. Test solutions of Au^{+} were prepared by
127 dilution of the stock (2.7 $g.L^{-1}$) in DMEM+FBS.

128 After the acclimatization period, fish were anesthetized with 100 $mg.L^{-1}$ tricaine
129 methanesulfonate (MS-222) and subsequently euthanized by spinal section. The
130 liver of each animal was carefully removed, washed with fresh phosphate-buffered
131 saline (PBS), cut into small cubes (2x2 mm) and cultured in an incubator at 25 °C
132 and 5% CO_2 during 24 h as previously reported (Oliveira et al. 2003). Per fish, six
133 liver cubes per experimental condition were considered. A total of 20 animals was
134 used in this experimental assay corresponding to 5 animals per test repetition (total
135 of tests: 4). The tested concentrations were: 4, 80, 1,600, 3,200, 4,200, 5,200, 6,200
136 and 7,200 $\mu g.L^{-1}$ of Au (ionic or nano form – 7 and 40 nm; citrate and PVP coating);
137 1.5, 15, 150, 1,500 and 15,000 $\mu g.L^{-1}$ of GEM and mixture of 80 $\mu g.L^{-1}$ of Au (ionic
138 or nano form) with 150 $\mu g.L^{-1}$ GEM. The lowest concentration of AuNPs (4 $\mu g.L^{-1}$)
139 was selected as a compromise between predicted values of AuNPs for the aquatic
140 environment (0.14 $\mu g.L^{-1}$) (García-Negrete et al., 2013; Tiede et al., 2009) and the
141 lowest Au concentration detectable limit in the experimental media. The other
142 AuNPs concentrations tested were progressive increases (e.g., 20 or 2-fold
143 increases. Two sizes and two coatings were selected to understand the correlation
144 between the nanoparticles characteristics and their toxic effects. The effects of Au^{+}
145 were also assessed to allow understanding the nanoparticle specific effect.

Concerning GEM, the lowest tested concentration was chosen based on levels detected in surface waters (Fang et al., 2012). The concentration range used to GEM was based on 10-fold increases. The concentrations GEM and Au used for the combined exposures were based on the effects detected in previous *in vivo* studies with *S. aurata* (Barreto et al. 2018, 2019a, 2019b, 2020). A negative control (only DMEM+FBS) and a solvent control with DMSO (at 0.03%, the highest concentration of DMSO used in the GEM treatments) were also performed. Immediately after liver sampling and before organ culture initiation, three liver cubes per fish were stored at -80 ºC until further processing. These samples were collected to determine the basal activities/levels of the liver for the assessed endpoints, corresponding to a time 0 h control. Samples of the experimental media were collected at 0 and 24 h for the quantification of Au and GEM. After 24 h exposure, six liver cubes per experimental condition, per fish, were collected: three for biochemical analysis (stored at -80 ºC until further processing) and three for DNA integrity assessment (immediately processed).

2.4. Quantification of gold and gemfibrozil (GEM) in the experimental media

The determination of Au in the experimental media was performed according to the NIST NCL Method PCC-8 (NIST 2010). After microwave assisted-acid digestion, sample solutions were analyzed by inductively coupled plasma mass spectrometry (ICP-MS) using an iCAP^{TM} Q ICP-MS equipment (Thermo Fisher Scientific). Elemental isotope – ^{197}Au – was monitored for analytical determination; ^{159}Tb and ^{209}Bi used as internal standards.

The GEM quantification was carried out by solid phase extraction (SPE) as sample preparation technic followed by liquid chromatography (HPLC) with fluorescence detector. SPE was performed using Oasis Strata-X cartridges (200 mg, 3 mL) from Phenomenex. Working standard solutions and extracts were analyzed using a Shimadzu LC system equipped with a SIL 20A autosampler, a DGU-20A5 degasser, a LC 20AB pump, and a RF-10AXL fluorescence detector. For the detection and quantification of GEM a Luna column (C18, 5 µm particle size, 4.60×150 mm, Phenomenex) was used. The optimal conditions were found using acetonitrile (eluent B) and 0.1% formic acid in ultrapure water (eluent A), a flow rate of 1.0 $mL.min^{-1}$, an oven temperature of 30 ºC, and an excitation/emission wavelength pair of 210/300 nm. The linear gradient program was run as 5 min from 50 to 100% (B) and after 4 min at 100% (B). Injection volume was 40 µL. More detailed information is presented in the Supplementary Information.

2.5. Biochemical analysis

Liver cubes were homogenized in potassium phosphate buffer (0.1 mM; pH 7.4), using an ultrasonic homogenizer (Branson Ultrasonics Sonifier S-250A). The resultant homogenate was divided in two aliquots: one for the evaluation of lipid peroxidation (LPO) levels and the other one for post-mitochondrial supernatant (PMS) isolation. To prevent oxidation, the aliquot of homogenate for LPO levels determination was transferred to a microtube with 4% BHT (2,6-Di-tert-butyl-4-methylphenol) in methanol and stored at -80 ºC until analysis. PMS was obtained by centrifugation (12,000 g; 20 min; 4 ºC) and aliquots were stored at -80 ºC until GST, CAT and GR activities assessment.

193 Protein concentration was determined according to Bradford (1976), adapted to
194 a microplate format, measuring the absorbance at 600 nm and using bovine γ-
195 globuline as a standard.
196 GST activity was determined according to the method of Habig et al. (1974),
197 adapted to a microplate format (Frasco and Guilhermino 2002), following the
198 conjugation of the substrate – 1-chloro-2, 4-dinitrobenzene (CDNB) – with reduced
199 glutathione. Absorbance was recorded at 340 nm and GST activity calculated as
200 nmol CDNB conjugate formed per min per mg of protein ($\varepsilon=9.6\times10^{-3}$ $M^{-1}.cm^{-1}$).
201 CAT activity was assessed according Claiborne (1985). The change in
202 absorbance at 240 nm caused by the dismutation of hydrogen peroxide (H_2O_2) was
203 recorded and CAT activity was evaluated in terms of μmol of H_2O_2 consumed per
204 min per mg of protein ($\varepsilon=40$ $M^{-1}.cm^{-1}$).
205 GR activity was evaluated by the method of Carlberg and Mannervik (1975)
206 adapted to a microplate format (Lima et al. 2007), measuring the reduced
207 nicotinamide-adenine dinucleotide phosphate (NADPH) disappearance at 340 nm
208 and expressed as nmol of oxidized NADPH ($NADP^+$) produced per min per mg of
209 protein ($\varepsilon=6.22\times10^{3}$ $M^{-1}.cm^{-1}$).
210 LPO levels were measured by the formation of thiobarbituric acid reactive
211 substances (TBARS) based on Ohkawa et al. (1979), adapted by Filho et al. (2001).
212 Absorbance was evaluated at 535 nm and LPO levels expressed as nmol of TBARS
213 produced per mg of protein ($\varepsilon=1.56\times10^{5}$ $M^{-1}.cm^{-1}$).
214
215 **2.6. DNA integrity assessment**

The alkaline comet assay was performed according to method of Singh et al. (1988) with some adaptations. Each liver cube was disrupted in PBS (pH 7.4) to obtain a suspension. This suspension was centrifuged, the supernatant was discarded, and the pellet was resuspended in fresh PBS. Then, cell suspension was added to 1% (w/v) low melting point agarose (at 40 ºC) and the mixture added to a microscope slide pre-coated with 1% (w/v) of normal melting point agarose. Solidification of agarose was allowed by keeping the slides on ice for 5 min. Positive controls (cell suspensions treated with 25 µM of H_2O_2 during 10 min) were included for each electrophoresis run to verify that the electrophoresis conditions were adequate. To lyse the cells, the slides were subsequently immersed in prepared ice-cold lysis solution (2.5 M NaCl, 100 mM EDTA and 10 mM Tris; pH 10.0) containing freshly added 1% Triton X-100 for 1 h, at 4 °C, in the dark. The slides were incubated in alkaline buffer (300 mM NaOH and 1 mM EDTA; pH>13) during 20 min for DNA unwinding. Electrophoresis was performed in the same buffer for 30 min by applying an electric field of 20 V and adjusting the current to 300 mA. After the electrophoresis, the slides were washed with 400 mM Tris-HCl buffer (pH 7.5). The slides were also dehydrated with absolute ethanol and left to dry in the dark. Slides were stained with ethidium bromide (20 $\mu L.mL^{-1}$), covered with a coverslip and then visualised using a fluorescence microscope (Olympus BX41TF) at 400X magnification.

Slides were analysed randomly, by counting one hundred cells per slide, arbitrarily selected. Cells were scored visually, according to tail length, into 5 classes – from class 0 to 4 (Collins 2004). A damage index (DI) expressed in arbitrary units

was assigned to each replicate and consequently for each treatment, according to the damage classes, applying the formula:

$$\mathrm{DI} = (0 \times \mathrm{n0}) + (1 \times \mathrm{n1}) + (2 \times \mathrm{n2}) + (3 \times \mathrm{n3}) + (4 \times \mathrm{n4})$$

where n = number of cells in each class analysed. DI can vary from 0 to 400.

2.7. Data analysis

First, Shapiro-Wilk and Levene's tests were used to assess the normality and homogeneity of variance of the data, using the Sigma Plot 12.0 software package. Differences between controls (negative and solvent) were examined using a Student t-test. To detect significant differences between the control and AuNPs single treatments, a two-way analysis of variance (ANOVA) was performed, using concentration and coating as factors, followed by a Dunnett's test. In addition, differences between Au^{+}, GEM, the mixtures and control were tested using a one-way ANOVA, followed by Dunnett's test. One-way ANOVA, followed by Tukey's test, whenever applicable, was used to compare differences between AuNPs, Au^{+} and GEM single treatments. Significant differences were accepted for $p<0.05$.

In the combined exposures, the observed effects (in percentage) were compared with the predicted effects (in percentage) obtained by the sum of single exposure effects. This analysis was performed to understand if the combined effect of Au (nano or ionic form) and GEM was lower, similar or greater than the sum of single exposure effects.

3. Results

3.1. Characterisation and behaviour of gold nanoparticles (AuNPs)

The synthesized cAuNPs displayed a round shape (Figure 1A and C), a well-defined absorption band and negative surface charge (Table S1) associated with the citrate layer. The analysis of the size, taking into account the results obtained by DLS and TEM images, revealed an expected average size around 7 and 40 nm. PVP coating led to an increased size due to a PVP layer, detectable by SEM in some AuNPs (Figure 1B and D). The UV-Vis spectra revealed a slight shift in surface plasmon resonance (SPR) peak to longer wavelength when compared with the original cAuNPs (Table S1). ZP shifted from -43 to around -13 mV and from -44 to -17 mV, for 7 and 40 nm AuNPs, respectively (Table S1).

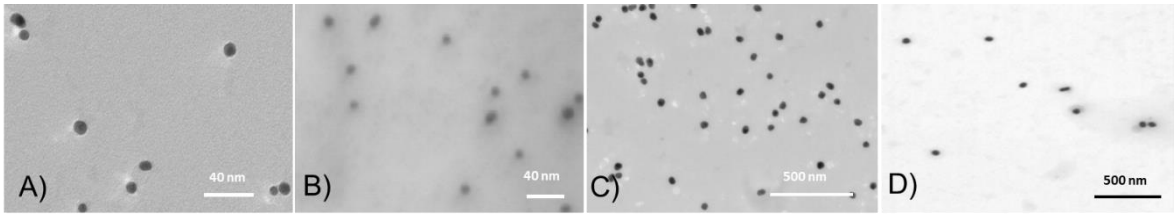

Figure 1. Electron microscopy images of 7 and 40 nm citrate (cAuNPs) and polyvinylpyrrolidone (PVP-AuNPs) gold nanoparticles stock suspensions in ultrapure water: **A)** 7 nm cAuNPs (100 $mg.L^{-1}$); **B)** 7 nm PVP-AuNPs (78 $mg.L^{-1}$); **C)** 40 nm cAuNPs (97 $mg.L^{-1}$); **D)** 40 nm PVP-AuNPs (58 $mg.L^{-1}$).

In ultrapure water, AuNPs were stable, with no detectable agglomerates/aggregates (Figure 1). Size, ZP and UV-Vis spectra of each type of AuNPs were similar during the assessed periods 0, 12 and 24 h. In DMEM+FBS, at 0 h, the characteristics of each type of AuNPs were similar to those in ultrapure water, with a slight less negative ZP, slight 1-4 nm increased sizes and shifted SPR

peaks toward higher wavelengths (increased about 2–4 nm). Within 12 h, for concentrations higher than 1,600 µg.L^{-1}, AuNPs aggregated/agglomerated, with sizes, assessed by DLS, bigger than 100 nm (Figure 2) and SPR peaks shifted toward higher wavelengths (Figure S1). Alterations in ZP were also found, with different peaks correspondent to different charges. After 24 h, no alterations in the size were found, comparing with 12 h (Figure 2) but the SPR peak disappeared (Figure S1).

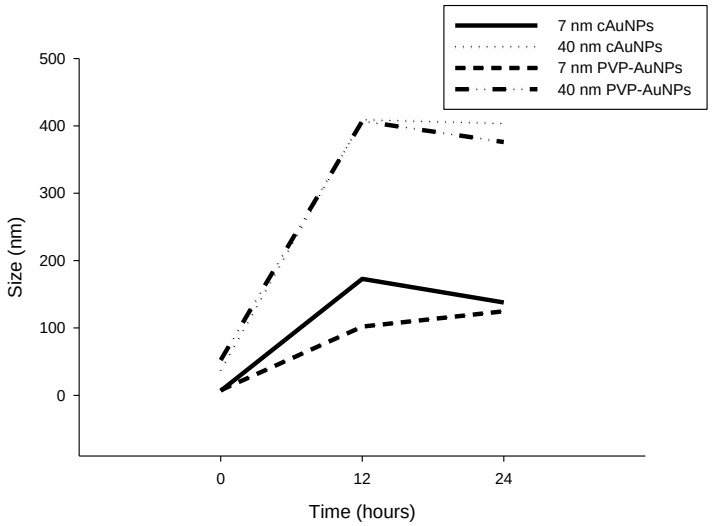

Figure 2. Size of gold nanoparticles (AuNPs), measured by dynamic light scattering (DLS), in Dulbecco's Modified Eagle's medium with fetal bovine serum (DMEM+FBS) at 0, 12 and 24 h. cAuNPs – Citrate coated gold nanoparticles; PVP-AuNPs – Polyvinylpyrrolidone coated gold nanoparticles.

The colour of the AuNPs in DMEM+FBS, at 12 h, was between red and blue, being bluer in the highest concentrations. At 24 h, some dark sediment was found in the bottom of the wells. This sediment increased with the increase of AuNPs concentration. At the lower tested concentrations (4 and 80 µg.L^{-1}), the media did not present the typical colour of AuNPs agglomeration/aggregation.

3.2. Quantification of gold and gemfibrozil (GEM) in the experimental media

At 0 h, in general, the amount of Au quantified in the experimental media (DMEM+FBS) was lower than the nominal concentrations. After 24 h of exposure, the concentration of Au decreased, particularly after exposure to AuNPs (Table S2). Concerning GEM, at 0 h, measured concentrations were lower than the nominal concentrations, with exception of the concentrations 1.5 and 15 $\mu g.L^{-1}$ – Table S2. After 24 h, the concentration of GEM decreased slightly.

3.3. Biological effects

For all the tested endpoints, no significant differences ($p>0.05$; t-test) were found between the samples collected immediately after liver sampling and before organ culture initiation (control at 0 h) and controls in DMEM+FBS after 24 h culture. Moreover, after 24 h liver organ culture, no significant differences were found between control and solvent control groups in terms of the tested endpoints ($p>0.05$; t-test). Therefore, the treatments were compared to the control.

3.3.1. Effects of 7 nm gold nanoparticles (AuNPs)

For the smallest tested AuNPs, coating promoted different response patterns. The cAuNPs only affected CAT activity at the highest concentration, increasing it ($p<0.05$; Dunnett's test), whereas almost all concentrations tested of PVP-AuNPs (except 4, 3,200 and 4,200 $\mu g.L^{-1}$) increased CAT activity ($p<0.05$; Dunnett's test; Figure 3A). At 80, 5,200 and 6,200 $\mu g.L^{-1}$, PVP-AuNPs increased significantly more the CAT activity than cAuNPs ($p<0.05$; Dunnett´s test; Figure 3A). Also, the highest concentrations (5,200, 6,200 and 7,200 $\mu g.L^{-1}$) increased significantly more the CAT

activity than the lowest concentrations (4 and 80 µg.L^{-1}) (p<0.05; Tukey's test; Figure 3A). In terms of GR, activity was increased after exposure to 3,200 and 5,200 µg.L^{-1} cAuNPs and to PVP-AuNPs, at concentrations higher than 80 µg.L^{-1} (p<0.05; Dunnett's test; Figure 3B). At 5,200 µg.L^{-1}, PVP-AuNPs increased significantly more the GR activity than cAuNPs (p<0.05; Dunnett´s test; Figure 3A). GST activity was not significantly affected by exposure to 7 nm AuNPs (p>0.05; ANOVA; Figure 3C).

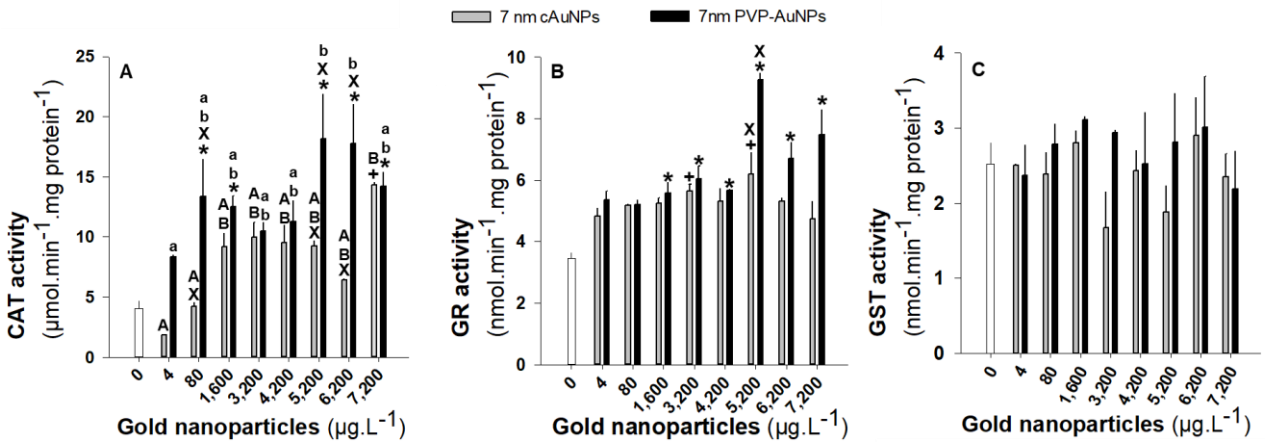

Figure 3. Catalase (CAT) **(A)**, glutathione reductase (GR) **(B)** and glutathione *S*-transferases (GST) **(C)** activities in *Sparus aurata* liver after 24 h organ culture exposure to 7 nm gold nanoparticles. Results are expressed as mean ± standard error. $^{+}$Significant differences to control (Dunnett's test, p<0.05, citrate coating). *Significant differences to control (Dunnett's test, p<0.05, polyvinylpyrrolidone coating). ^{X}Significant differences between cAuNPs and PVP-AuNPs within the same concentration (Dunnett's test, p<0.05). Different letters correspond to significant differences between the concentrations of each type of AuNPs, capital letters to cAuNPs and small letters to PVP-AuNPs (Tukey's test, p<0.05). Citrate coated gold nanoparticles – cAuNPs; Polyvinylpyrrolidone coated gold nanoparticles – PVP-AuNPs.

The 7 nm AuNPs displayed ability to induce peroxidative damage in membranes. This effect was more consistent for PVP-AuNPs, that induced increased TBARS at concentrations higher than 4,200 µg.L^{-1} whereas for cAuNPs, effects were only found at 3,200 µg.L^{-1} (p<0.05; Dunnett's test; Figure 4A). Indeed, at 5,200 and 6,200 µg.L^{-1}, PVP-AuNPs induced significantly higher levels of peroxidative damage than cAuNPs (p<0.05; Dunnett's test; Figure 4A). At 5,200 and 6,200 µg.L^{-1}, PVP-AuNPs induced significantly higher levels of LPO than at 4 to 4,200 µg.L^{-1} (p<0.05; Tukey's test; Figure 4A). All the 7 nm AuNPs tested concentrations induced DNA damage (p<0.05; Dunnett's test; Figure 4B), with 5,200 and 7,200 µg.L^{-1} inducing significantly more DNA damage than 4 µg.L^{-1} (p<0.05; Tukey's test; Figure 4B).

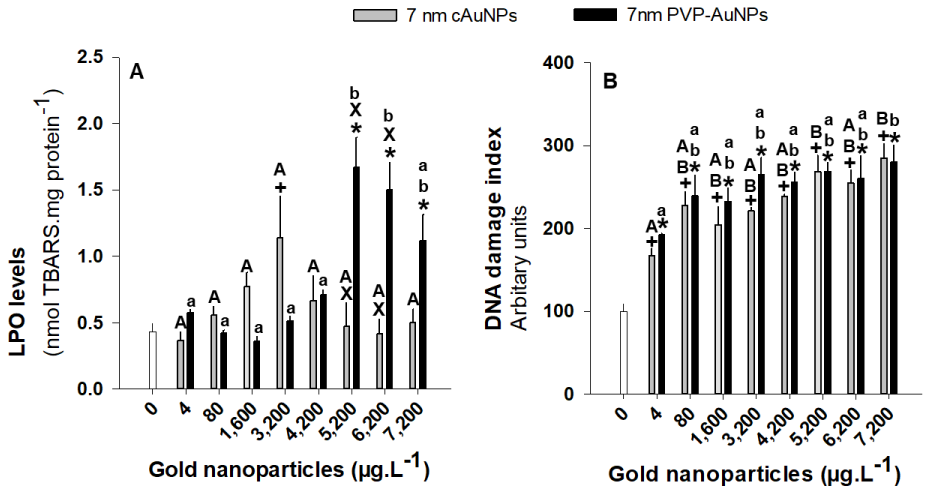

Figure 4. Lipid peroxidation (LPO) levels **(A)** and DNA damage index **(B)** of *Sparus aurata* liver after 24 h organ culture exposure to 7 nm gold nanoparticles. Results are expressed as mean ± standard error. $^{+}$Significant differences to control (Dunnett's test, p<0.05, citrate coating). *Significant differences to control (Dunnett's test, p<0.05, polyvinylpyrrolidone coating). ^{X}Significant differences between cAuNPs and PVP-AuNPs within the same concentration (Dunnett's test, p<0.05).

Different letters correspond to significant differences between the concentrations of each type of AuNPs, capital letters to cAuNPs and small letters to PVP-AuNPs (Tukey's test, $p<0.05$). Citrate coated gold nanoparticles – cAuNPs; Polyvinylpyrrolidone coated gold nanoparticles – PVP-AuNPs.

3.3.2. Effects of 40 nm gold nanoparticles (AuNPs)

Effects of 40 nm AuNPs on CAT activity were found, for both coatings, at concentrations higher than 3,200 µg.L^{-1} ($p<0.05$; Dunnett's test; Figure 5A). The highest tested concentrations (4,200 to 7,200 µg.L^{-1}) increased significantly more the CAT activity than the lowest tested concentrations (4 to 3,200 µg.L^{-1}) ($p<0.05$; Tukey's test; Figure 5A). These particles also induced an increase in GR activity at 4,200 µg.L^{-1} for cAuNPs and concentrations higher than 1,600 µg.L^{-1} for PVP-AuNPs ($p<0.05$; Dunnett's test; Figure 5B). As observed in liver culture exposed to 7 nm AuNPs, GST activity was not significantly affected by 40 nm AuNPs ($p>0.05$; ANOVA; Figure 5C).

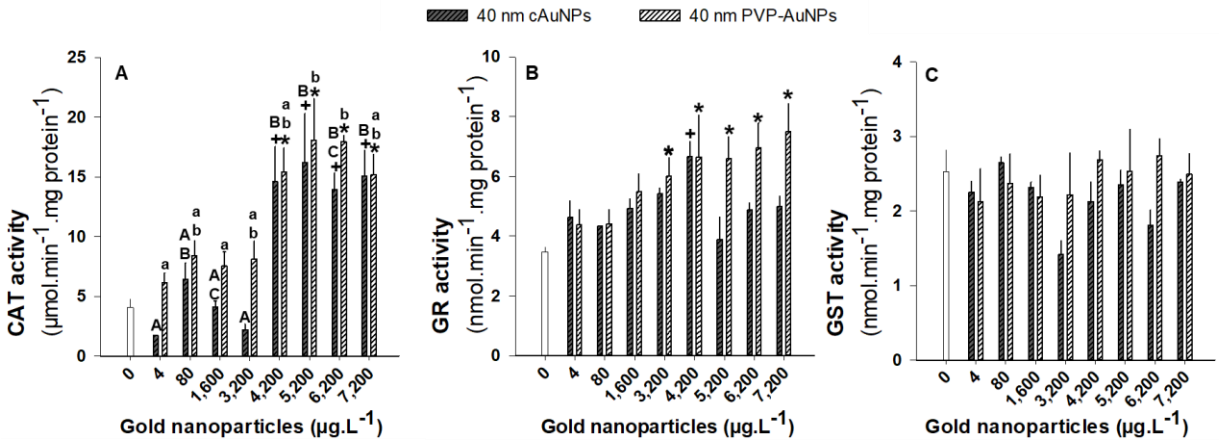

Figure 5. Catalase (CAT) **(A)**, glutathione reductase (GR) **(B)** and glutathione *S*-transferases (GST) **(C)** activities of *Sparus aurata* liver after 24 h organ culture

exposure to 40 nm gold nanoparticles. Results are expressed as mean ± standard error. $^{+}$Significant differences to control (Dunnett's test, p<0.05, citrate coating). *Significant differences to control (Dunnett's test, p<0.05, polyvinylpyrrolidone coating). Different letters correspond to significant differences between the concentrations of each type of AuNPs, capital letters to cAuNPs and small letters to PVP-AuNPs (Tukey's test, p<0.05). Citrate coated gold nanoparticles – cAuNPs; Polyvinylpyrrolidone coated gold nanoparticles – PVP-AuNPs.

No significant oxidative damage, assessed as LPO, was found after liver exposure to 40 nm AuNPs (p>0.05; ANOVA; Figure 6A). However, DNA damage was found after exposure to concentrations higher than 4 µg.L^{-1} for PVP-AuNPs and 80 µg.L^{-1} for cAuNPs (p<0.05; Dunnett's test; Figure 6B). The highest tested concentrations (e.g., 3,200 to 7,200 µg.L^{-1} cAuNPs) induced significantly more DNA damage when compared with the lowest tested concentrations (e.g., 4 and 80 µg.L^{-1} cAuNPs) (p<0.05; Tukey's test; Figure 6B).

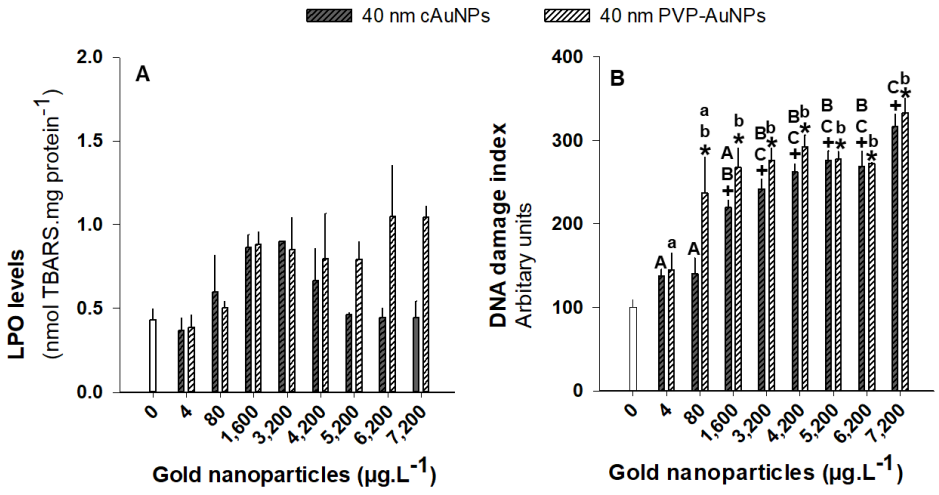

Figure 6. Lipid peroxidation (LPO) levels **(A)** and DNA damage index **(B)** of *Sparus aurata* liver after 24 h organ culture exposure to 40 nm gold nanoparticles. Results are expressed as mean ± standard error. $^{+}$Significant differences to control (Dunnett's test, $p<0.05$, citrate coating). *Significant differences to control (Dunnett's test, $p<0.05$, polyvinylpyrrolidone coating). Different letters correspond to significant differences between the concentrations of each type of AuNPs, capital letters to cAuNPs and small letters to PVP-AuNPs (Tukey's test, $p<0.05$). Citrate coated gold nanoparticles – cAuNPs; Polyvinylpyrrolidone coated gold nanoparticles – PVP-AuNPs.

3.3.3. Effects of ionic gold (Au^{+})

At concentrations higher than 3,200 µg.L^{-1}, Au^{+} significantly increased the activities of CAT and GR ($p<0.05$; Dunnett's test; Figure 7A and B). The highest tested concentrations (4,200 to 7,200 µg.L^{-1}) increased significantly more the CAT activity than the lowest tested concentrations (4 to 1,600 µg.L^{-1}) ($p<0.05$; Tukey's test; Figure 7A). As observed for AuNPs, liver exposure to Au^{+} did not induce significant alterations in GST activity ($p>0.05$; ANOVA; Figure 7C).

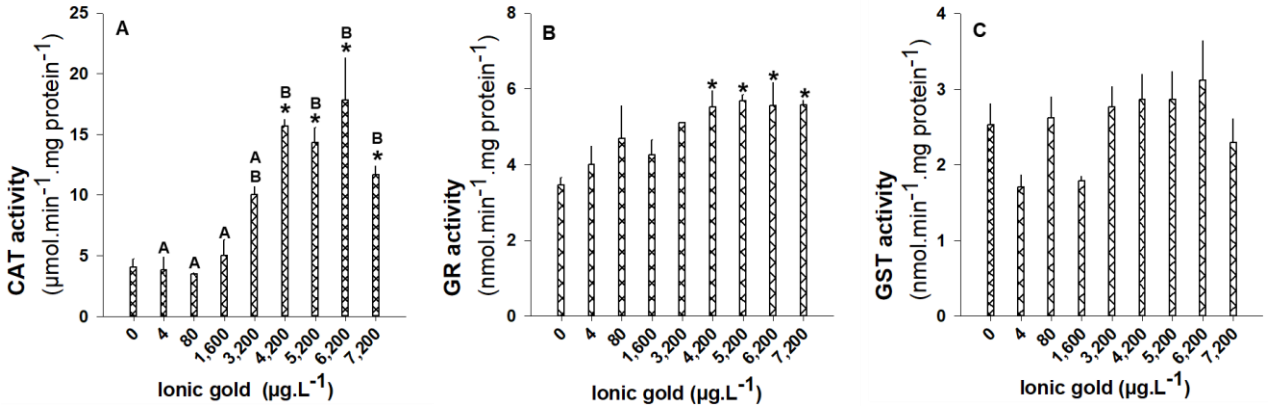

Figure 7. Catalase (CAT) **(A)**, glutathione reductase (GR) **(B)** and glutathione S-transferases (GST) **(C)** activities of *Sparus aurata* liver after 24 h organ culture exposure to ionic gold. Results are expressed as mean ± standard error. *Significant differences to control (Dunnett's test, $p<0.05$). Different letters correspond to significant differences between the concentrations (Tukey's test, $p<0.05$).

The LPO levels remained unchanged after the exposure to Au^{+} ($p>0.05$; ANOVA; Figure 8A). However, DNA damage was found after exposure to all the tested concentrations ($p<0.05$; Dunnett's test; Figure 8B). The highest tested concentrations (e.g., 6,200 and 7,200 µg.L^{-1}) induced significantly more DNA damage when compared with the lowest tested concentrations (e.g., 4 to 1600 µg.L^{-1} cAuNPs) ($p<0.05$; Tukey's test; Figure 8B).

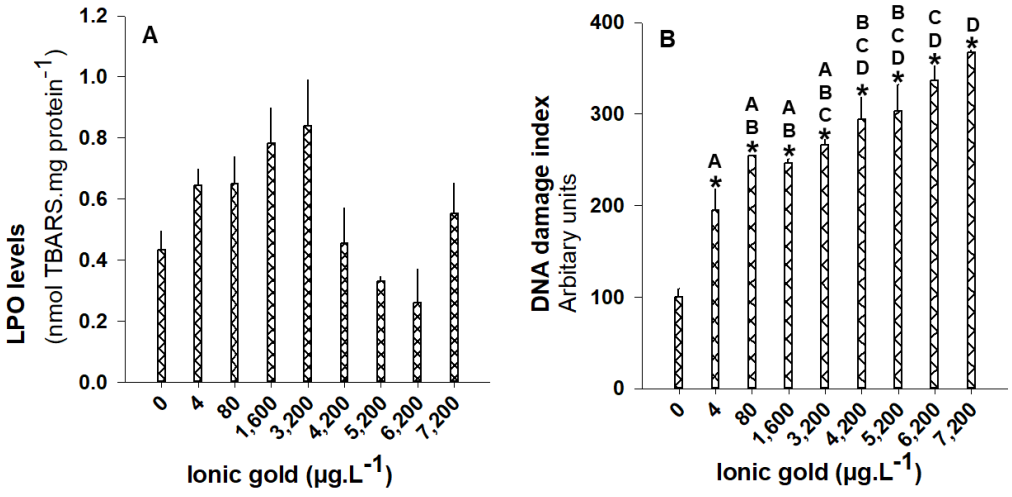

Figure 8. Lipid peroxidation (LPO) levels **(A)** and DNA damage index **(B)** of *Sparus aurata* liver after 24 h organ culture exposure to ionic gold. Results are expressed as mean ± standard error. *Significant differences to control (Dunnett's

test, $p<0.05$). Different letters correspond to significant differences between the concentrations (Tukey's test, $p<0.05$).

3.3.4. Effects of gemfibrozil (GEM)

CAT and GR activities were significantly increased after exposure to 15,000 µg.L^{-1} GEM ($p<0.05$; Dunnett's test; Figure 9A and B). GEM, at 15,000 µg.L^{-1}, significantly increased CAT activity comparing with the other tested concentrations (1.5 to 1,500 µg.L^{-1}) ($p<0.05$; Tukey's test; Figure 9A). However, GST activity was not significantly affected by exposure to GEM ($p>0.05$; ANOVA; Figure 9C).

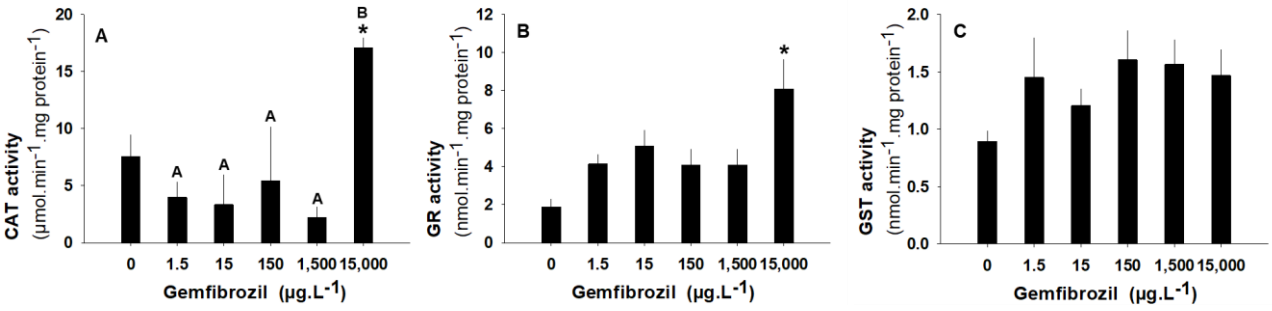

Figure 9. Catalase (CAT) **(A)**, glutathione reductase (GR) **(B)** and glutathione *S*-transferases (GST) **(C)** activities of *Sparus aurata* liver after 24 h organ culture exposure to gemfibrozil. Results are expressed as mean ± standard error. *Significant differences to control (Dunnett's test, $p<0.05$). Different letters correspond to significant differences between the concentrations (Tukey's test, $p<0.05$).

LPO levels significantly increased after exposure to 15,000 µg.L^{-1} GEM ($p<0.05$; Dunnett's test; Figure 10A). GEM, at 15,000 µg.L^{-1}, induced significantly higher levels of LPO than 1.5, 150 and 1,500 µg.L^{-1} GEM ($p<0.05$; Tukey's test; Figure

10A). In terms of DNA damage, all tested GEM concentrations led to a significant decrease in the DNA integrity (p<0.05; Dunnett's test; Figure 10B). The highest tested concentrations, 1,500 and 15,000 µg.L^{-1}, induced significantly more DNA damage than the lowest tested concentrations (1.5 to 150 µg.L^{-1} cAuNPs) (p<0.05; Tukey's test; Figure 10B).

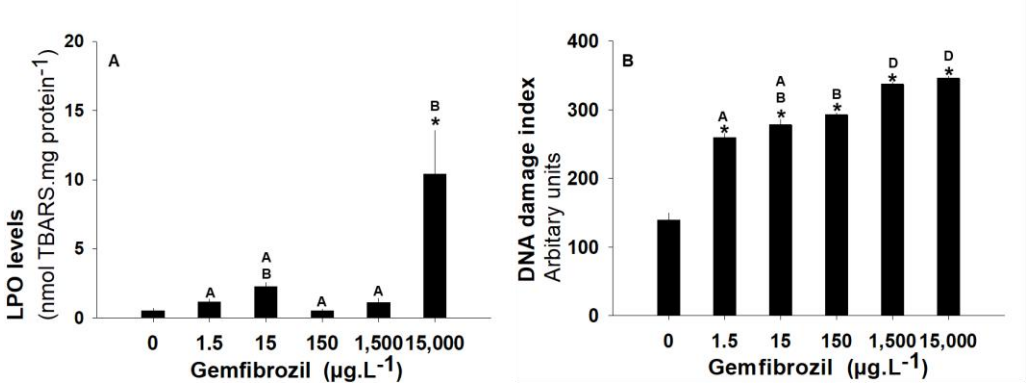

Figure 10. Lipid peroxidation (LPO) levels **(A)** and DNA damage index **(B)** of *Sparus aurata* liver after 24 h organ culture exposure to gemfibrozil. Results are expressed as mean ± standard error. *Significant differences to control (Tukey's test, p<0.05). Different letters correspond to significant differences between the concentrations (Tukey's test, p<0.05).

3.3.5. Effects of combined exposures: gold and gemfibrozil (GEM)

In the combined exposures, CAT activity significantly increased (p<0.05; Dunnett's test; Figure 11A), with observed percentages of effect being higher than the predicted based on the single exposures (Table 1). The combined exposures to Au^{+} + GEM and 40 nm PVP-AuNPs + GEM significantly increased GR activity (p<0.05; Dunnett's test; Figure 11B), with observed percentages of effect being higher than the predicted (Table 1). GST activity was not significantly affected by the combined exposures (p>0.05; ANOVA; Figure 11C), as observed in the single

exposures. For this endpoint, the observed percentages of effect were the predicted (Table 1).

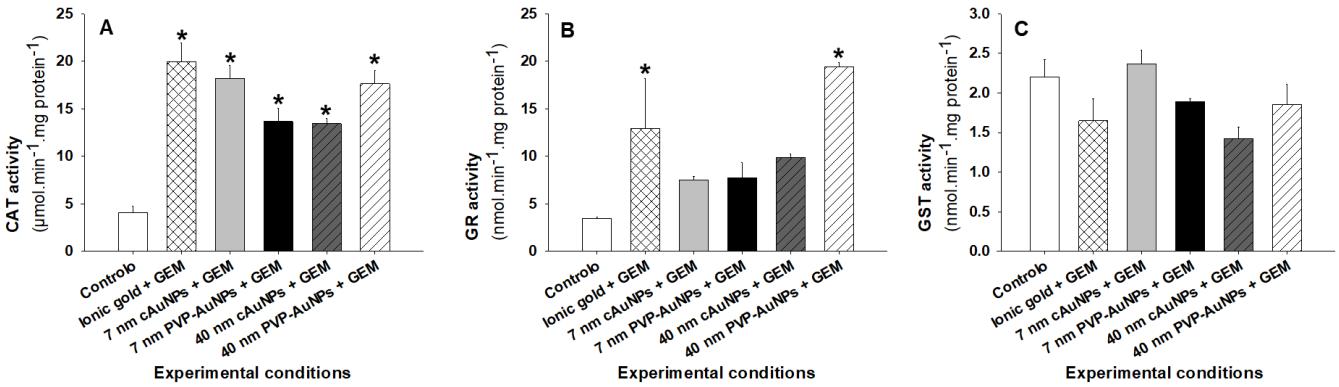

Figure 11. Catalase (CAT) **(A)** glutathione reductase (GR) **(B)** and glutathione *S*-transferases (GST) **(C)** activities of *Sparus aurata* liver after 24 h organ culture combined exposure to gold nanoparticles (AuNPs) or ionic gold (Au^{+}) with gemfibrozil (GEM). Results are expressed as mean ± standard error. *Significant differences to control (Dunnett´s test, $p<0.05$). Citrate coated gold nanoparticles – cAuNPs; Polyvinylpyrrolidone coated gold nanoparticles – PVP-AuNPs; Au + GEM – 80 µg.L^{-1} Au^{+} or AuNPs (cAuNPs or PVP-AuNPs) with 150 µg.L^{-1} GEM.

The combined exposures to PVP-AuNPs (7 and 40 nm) and GEM significantly increased LPO levels ($p<0.05$; Dunnett's test; Figure 12A), yielding observed percentages of effect higher than the predicted (Table 1). All the combined exposures induced significant increases in DNA damage ($p<0.05$; Dunnett's test; Figure 12B), with the observed percentages of effect similar to those expected (Table 1).

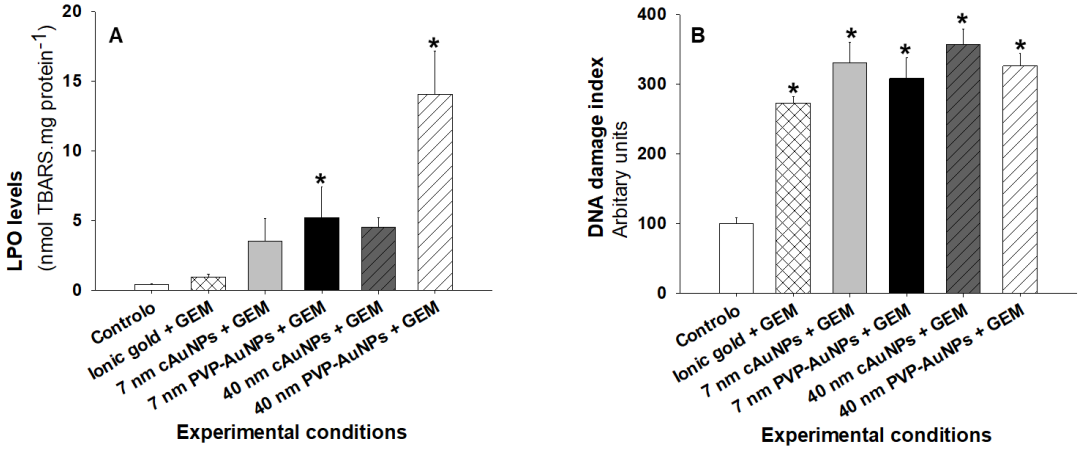

493

494 **Figure 12.** Lipid peroxidation (LPO) levels **(A)** and DNA damage index (arbitrary
495 units) **(B)** of *Sparus aurata* liver after 24 h organ culture combined exposure to gold
496 nanoparticles (AuNPs) or ionic gold (Au^{+}) with gemfibrozil (GEM). Results are
497 expressed as mean ± standard error. *Significant differences to control (Dunnett´s
498 test, p<0.05). Citrate coated gold nanoparticles – cAuNPs; Polyvinylpyrrolidone
499 coated gold nanoparticles – PVP-AuNPs; Au + GEM – 80 $\mu g.L^{-1}$ Au^{+} or AuNPs
500 (cAuNPs or PVP-AuNPs) with 150 $\mu g.L^{-1}$ GEM.

Table 1. The relative percentage of effect in the different assessed endpoints, after 24 h liver organ culture single and combined exposures to 80 µg.L^{-1} gold nanoparticles (citrate coated – cAuNPs and polyvinylpyrrolidone coated – PVP-AuNPs), 80 µg.L^{-1} ionic gold (Au^{+}) and 150 µg.L^{-1} gemfibrozil (GEM) compared with control. Observed **(O)** % in the combined exposures refers to measured effects and the Predicted **(P)** % were derived by the sum of single exposure effects. *****Significant differences to control (Dunnett´s test, $p<0.05$).

Assessed Endpoints	**% of effect related to control**										
	Au^{+}	**7 nm cAuNPs**	**7 nm PVP-AuNPs**	**40 nm cAuNPs**	**40 nm PVP-AuNPs**	**GEM**	**Au^{+} + GEM**	**7 nm cAuNPs + GEM**	**7 nm PVP-AuNPs + GEM**	**40 nm cAuNPs + GEM**	**40 nm PVP-AuNPs + GEM**
Catalase Activity	40	27	- 131 *	-11	-45	6	P: 46 O: - 244 *	P: 33 O: - 213 *	P: - 124 O: - 136 *	P: - 5 O: - 132 *	P: - 39 O: - 204 *
Glutathione Reductase Activity	- 57	- 73	- 74	- 44	- 47	- 37	P: - 94 O: - 333 *	P: - 110 O: - 150	P: - 111 O: - 159	P: - 81 O: - 231	P: - 84 O: - 549 *
Glutathione *S*-Transferases Activity	- 69	- 54	- 80	- 71	- 53	- 4	P: - 73 O: - 7	P: - 58 O: - 53	P: - 84 O: - 22	P: - 74 O: - 8	P: - 57 O: -20
Lipid Peroxidation Levels	- 42	- 22	8	- 31	- 10	- 14	P: - 57 O: - 114	P: - 36 O: - 679	P: - 7 O: - 1048 *	P: - 45 O: - 896	P: - 24 O: - 2988 *
DNA Damage Index	- 128 *	- 104 *	- 115 *	- 26	- 112 *	- 162 *	P: - 290 O: - 145 *	P: -266 O: - 197 *	P: - 277 O: - 177 *	P: - 188 O: - 221 *	P: - 274 O: - 193 *

4. Discussion

In the present study, the agglomeration/aggregation of AuNPs found within 12 h in DMEM+FBS may influence the nanoparticles (NPs) toxicity. Several research groups already reported that aggregation of NPs in cell culture media or PBS might be prevented by adding serum, presumably due to proteins adsorbing onto the particle surface (Allouni et al. 2009; Barreto et al. 2015; Balog et al. 2015; Bihari et al. 2008; Mahl et al. 2010, 2012). Barreto et al. (2015) reported that cAuNPs immediately aggregated/agglomerated in DMEM whereas in DMEM+FBS they were stable for 12 hours. In the present study, at 0 h, in DMEM+FBS, the size of AuNPs increased (although non-significantly), the SPR peaks shifted toward higher wavelengths and ZP values were slightly less negative, as previously reported (Barreto et al. 2015). This suggests that FBS was bound to AuNPs, a relevant feature to take into consideration because, as previously reported, the attachment of FBS with NPs may influence its incorporation into the cells/organs and consequently reduce NPs toxic effects (Durán et al. 2015). Considering the effect of AuNPs concentration on the behaviour of the particles, it was observed that the time needed for AuNPs to aggregate/agglomerate in the DMEM+FBS decreased with the increase of AuNPs concentration. This is an expected finding because with the increasing number of particles per volume, the probability of NPs collisions and consequent agglomeration/aggregation will increase (Barreto et al. 2015). At 12 h, the medium (DMEM+FBS with AuNPs) was bluer at the highest concentrations of AuNPs, corroborating the previously described information. According to Zeng et al. (2012), the surface energy of AuNPs increases with the decrease of the diameter. Therefore, smaller AuNPs interact more strongly with the compounds

present in the solution, leading to size-dependent aggregation of AuNPs (Zeng et al. 2012). In the present study, this was not visually observed. Additionally, at 12 h, all 7 and 40 nm AuNPs already had aggregated/agglomerated. Thus, for the same concentration, the tested AuNPs sizes displayed similar behaviour in the test media, in terms of aggregation/agglomeration and stability period. However, different sizes of aggregates/agglomerates were detected, depending on the initial size of AuNPs, with aggregates/agglomerates resultant from 40 nm AuNPs being bigger than those resultant from 7 nm AuNPs.

Regarding Au concentration in the medium, at 24 h, a marked decrease was observed after exposure to AuNPs. This may be explained by the aggregation/agglomeration of the NPs and subsequent sedimentation of the aggregates/agglomerates.

In the available literature, AuNPs toxicity data are often conflicting due to the variability of the toxicity assays used in terms of cell lines, exposure times, assessed endpoints, NPs concentrations and chemical/physical properties. AuNPs have been reported as “nontoxic” according to some *in vitro* tests (Alkilany and Murphy 2010; Connor et al. 2005; Luis et al. 2016; Shukla et al. 2005). Shukla et al. (2005), using RAW264.7 macrophage murine cell line, reported that AuNPs (size range from 3 to 8 nm; concentrations between 10 and 100 μM) are not cytotoxic, reducing the production of reactive oxygen and nitrite species and not eliciting secretion of proinflammatory cytokines, making them suitable candidates for nanomedicine. Connor et al. (2005) reported that 18 nm AuNPs exposure did not cause acute cytotoxicity in human K562 cells, at concentrations up to 250 μM. Luis et al. (2016) also demonstrated *in vitro* that 7 nm AuNPs (concentrations between 54 $ng.L^{-1}$ to 2.5 $mg.L^{-1}$) did not affect *Mytilus galloprovincialis*

haemolymph' acetylcholinesterase nor gills' GST activities. However, other authors have reported that AuNPs may present toxicity (Baharara et al. 2016; Goodman et al. 2004; Li et al. 2010; Pan et al. 2009; Tkachenko et al. 2004). AuNPs (20 nm; 1 nM) induced autophagy with oxidative stress in MRC-5 human lung fibroblasts (Li et al. 2010). The investigation of Baharara et al. (2016) demonstrated the induction of apoptosis in human HeLa cell line treated with 100 and 400 $\mu g.mL^{-1}$ AuNPs (size range from 10 to 42 nm). HeLa and 3T3/NIH mouse embryo fibroblast cell lines exposed to AuNPs (20 nm; 0.98 nM) presented decreased cell viabilities (Tkachenko et al. 2004).

As previously reported, the possible adverse effects of AuNPs may be attributed to: 1) their interaction with the cell membrane (Goodman et al. 2004); 2) oxidative stress leading to cytotoxicity effects (Pan et al. 2009); 3) the inhibition of metabolic activity (e.g., leading to mitochondrial damage; Panessa-Warren et al. 2008); 4) possible damage or alteration in the nuclear DNA (Panessa-Warren et al. 2008; Schulz et al. 2012). In the current study, AuNPs induced oxidative stress and damage to different cellular components (DNA strand breaks and lipid membrane peroxidation), even at low concentrations (4 $\mu g.L^{-1}$), with effects dependent on the AuNPs size, coating and concentration. The 7 nm AuNPs induced more effects than 40 nm AuNPs. Only 7 nm AuNPs increased LPO levels. At 4 $\mu g.L^{-1}$, only 7 nm AuNPs caused DNA damage. This may be explained by the higher ability of 7 nm AuNPs to be incorporated by the cell comparing with 40 nm AuNPs. An *in vivo* genotoxic effect of different sizes of AuNPs (2, 20 and 200 nm) was observed by Schulz et al. (2012) in the lungs of rats, with DNA damage presenting a weak size-related increase of the mean tail intensity (Schulz et al. 2012). As previously described, 15 nm AuNPs *in vitro* permeation on rat

skin was higher and more rapid than 102 and 198 nm AuNPs (Sonavane et al. 2008). In the present study, the 7 nm PVP-AuNPs, which presented the smallest sizes during the experimental test, were those inducing more pronounced effects in the liver. For instance, 7 nm PVP-AuNPs induced significantly higher levels of peroxidative damage than cAuNPs. Comparing 40 nm cAuNPs and PVP-AuNPs, the latter also induced effects (for instance DNA integrity loss) at concentrations lower than those induced by cAuNPs. Previous studies also reported different effects of AuNPs with different coatings (Iswarya et al. 2016; Fraga et al. 2013; Paino et al. 2012). In a mice model, 96 h exposure to 65 nm PVP-AuNPs induced more effects in the DNA of liver cells (assessed as DNA strand breaks) than 29 nm cAuNPs (Iswarya et al. 2016). In the present study, in general, the toxicity of AuNPs was dependent on concentration of nanoparticles, with the highest tested concentrations inducing more effects than the lowest tested concentrations, regardless of the coating and size of AuNPs.

Comparing the present *in vitro* results with those obtained in *in vivo* exposures of *S. aurata* to AuNPs (Barreto et al. 2019b, 2020), some similar trends were observed, namely in terms of increases of CAT and GR activities, despite differences in the exposure length (*in vitro*: 24 h and *in vivo*: 96 h). However, some dissimilar results were also detected. For instance, GST activity was not altered after *in vitro* exposures whereas *in vivo* exposure of 1,600 $\mu g.L^{-1}$ 40 nm PVP-AuNPs increased hepatic GST activity (Barreto et al. 2019b). LPO levels were not altered *in vitro* in the range of concentrations 4 to 1,600 $\mu g.L^{-1}$ although 1,600 $\mu g.L^{-1}$ of 7 nm cAuNPs increased *in vivo* liver LPO levels (Barreto et al. 2020). Another interesting finding is that 7 nm cAuNPs were the ones inducing more adverse effects to *S. aurata* after *in vivo* exposure (Barreto et al. 2020)

whereas 7 nm PVP-AuNPs were the ones inducing more adverse effects to liver organ culture of *S. aurata*. These dissimilar results may be due to aggregation/agglomeration state of AuNPs dependent on the medium where they are present and the time of exposure. In addition, in the *in vivo* tests the whole living organism is used, and a range of mechanisms can occur in different tissues/organs to protect/eliminate a contaminant whereas in the *in vitro* test, only the mechanisms involved in cell, tissue or organ used are evaluated (i.e. the *in vitro* models do not represent all the complexity found in an *in vivo* model). Therefore, the results may not be always equivalent.

In the present work, gold in the nano form induced more adverse effects in the liver organ culture of *S. aurata* than the ionic form. Oxidative damage was only detected after the exposure to AuNPs. In agreement with the described results, the study of Barbasz and Oćwieja (2016), using two types of human cell lines, reported a higher cytotoxicity of AuNPs than Au^{+} (Barbasz and Oćwieja 2016). However, other studies reported a higher toxicity of Au^{+} comparing with AuNPs (Farkas et al. 2010; Luis et al. 2016). Farkas et al. (2010) reported that, in rainbow trout (*Oncorhynchus mykiss*) hepatocyte cells, the *in vitro* exposure to 17.4 $mg.L^{-1}$ Au^{+} significantly increased ROS levels. At the same concentration, AuNPs did not have any effect (Farkas et al. 2010). Luis et al. (2016) in another *in vitro* test also showed that Au^{+} significantly decreased the haemolymph' acetylcholinesterase and gills' GST activities of mussel *Mytilus galloprovincialis*. However, no significant alterations were found after *in vitro* exposure to AuNPs, regardless of their coating (Luis et al. 2016). A previous 96 h *in vivo* study with *S. aurata* also showed the highest toxicity of Au^{+} comparing with AuNPs (Barreto et al. 2020). There are few available studies about the possible mechanisms of Au^{+}

toxic action. Nonetheless, the Au^{+} ability to undergo redox reactions with peptides and proteins, particularly involving sulfur amino acids, to deprotonate and bind to peptide amide bonds and cross-link histidine imidazole rings has been reported (Best and Sadler 1996; Luis et al. 2016). Dissolution can play a critical role in the fate, behaviour and toxicity of NPs. Some NPs can dissolve quickly in aqueous media and the toxicity of some metal-based NPs, such as zinc oxide NPs and silver NPs, results from the metal ions released. Contrary, AuNPs are insoluble and its toxicity is not associated with the release of ions (Peng et al. 2017).

GEM exposure increased CAT and GR activities and LPO levels at the highest tested concentration but affected the DNA integrity at all the tested concentrations. *In vitro* toxicity of GEM was previously reported in the hepatoma fish cell line PLHC-1 (Zurita et al. 2007) manifested through a reduced protein content, neutral red uptake, methylthiazol metabolization and lysosomal function. *In vivo*, 96 h of GEM exposure increased *S. aurata* hepatic CAT (at 15,000 $\mu g.L^{-1}$) and GR (from 15 to 15,000 $\mu g.L^{-1}$) activities and LPO levels (at 1.5 $\mu g.L^{-1}$) (Barreto et al. 2018).

The effects of the concomitant exposure to AuNPs and GEM were, for many endpoints, higher than the predicted. A previous 96 h *in vivo* study also showed that the effects on *S. aurata* hepatic CAT and GR activities of the combined exposures – 40 nm AuNPs with GEM – were higher than the sum of the effects of each contaminant alone (Barreto et al. 2019b). The prediction of potential synergistic effects between AuNPs and GEM, found in the present study, is a relevant finding considering that, in the environment, there is a variety of contaminants that may interact with each other. To our best knowledge, a single *in vitro* study has so far assessed the combined effects of AuNPs and

pharmaceuticals (carbamazepine and fluoxetine) in aquatic organisms (Luis et al. 2016). It was demonstrated that AuNPs, in combined exposures, may significantly alter the effects of the pharmaceuticals carbamazepine and fluoxetine, even at concentrations that may be considered environmentally relevant. These effects were dependent on the coating of NPs and tested endpoint. In the present study, the detected effects of the combined exposures were also dependent on the characteristics of AuNPs, with 40 nm PVP-AuNPs with GEM inducing more synergistic effects than 40 nm cAuNPs combined with GEM and 7 nm AuNPs plus GEM.

The liver organ culture of *Sparus aurata* was sensitive to low concentrations of the tested contaminants and allowed to differentiate responses to NPs with different characteristics: size and coating. They also allowed the study of combined exposures, proving sensitive in discriminating experimental conditions. Taking into account that the organ cultures involve “the maintenance or growth of tissues, organ primordia or the whole or parts of an organ *in vitro* for a period of 24 h or longer, in a way which may allow differentiation and/or preservation of architecture and/or function” (Oliveira et al. 2003), this approach showed to be very useful, supporting its use as an *in vitro* model. Further studies, analysing different types of contaminants, are encouraged to understand if the liver organ culture can be used as an alternative to *in vivo* testing.

5. Conclusions

The *in vitro* system used in the present study proved to be a valuable approach to evaluate the single and combined effects of contaminants, such as nanoparticles and pharmaceuticals, to aquatic organisms. Gold nanoparticles

(AuNPs) induced oxidative stress, increasing the activities of catalase and glutathione reductase, and damage in DNA and cellular membranes, even at low concentrations (4 $\mu g.L^{-1}$), in the liver organ culture of *Sparus aurata*. The effects were dependent on the size, coating and concentration of AuNPs, being the 7 nm PVP-AuNPs that induced higher effects. Gold in the nano form caused more adverse effects than the ionic form of the metal. Additionally, gemfibrozil (GEM) also induced DNA damage at an environmental relevant concentration (1.5 $\mu g.L^{-1}$). In many endpoints, the combined exposures of AuNPs and GEM induced higher effects than the predicted, being an important finding considering that, in the environment, there is a diversity of contaminants that may interact with each other.

Conflict of interest statement

The authors declare that there are no conflicts of interest.

Acknowledgments

Thanks are due for the financial support to CESAM (UID/AMB/50017/2019), to FCT/MCTES through national funds, and the co-funding by the FEDER, within the PT2020 Partnership Agreement and Compete 2020. This research was supported through the COMPETE – Operational Competitiveness Program and national funds through FCT, under the project “NANOAu – Effects of Gold Nanoparticles to Aquatic Organisms” (FCT PTDC/MAR-EST/3399/2012) (FCOMP-01-0124-FEDER-029435), through FCT/MCTES through national funds (PIDDAC), the cofounding by FEDER, within the PT2020 Partnership Agreement and Compete 2020. A. Barreto has a doctoral fellowship from FCT

(SFRH/BD/97624/2013). M. Oliveira has financial support of the program Investigator FCT, co-funded by the Human Potential Operational Programme and European Social Fund (IF/00335(2015)).

6. References

Alkilany, A. M., and C. J. Murphy. 2010. 'Toxicity and cellular uptake of gold nanoparticles: what we have learned so far?', *Journal of Nanoparticle Research*, 12: 2313-33.

Allouni, Z. E., M. R. Cimpan, P. J. Høl, T. Skodvin, and N. R. Gjerdet. 2009. 'Agglomeration and sedimentation of TiO_2 nanoparticles in cell culture medium', *Colloids and Surfaces B: Biointerfaces*, 68: 83-87.

Baharara, J., T. Ramezani, A. Divsalar, M. Mousavi, and A. Seyedarabi. 2016. 'Induction of apoptosis by green synthesized gold nanoparticles through Activation of caspase-3 and 9 in human cervical cancer cells', *Avicenna Journal of Medical Biotechnology*, 8: 75-83.

Balog, S., L. Rodriguez-Lorenzo, C. A. Monnier, M. Obiols-Rabasa, B. Rothen-Rutishauser, P. Schurtenberger, and A. Petri-Fink. 2015. 'Characterizing nanoparticles in complex biological media and physiological fluids with depolarized dynamic light scattering', *Nanoscale*, 7: 5991-97.

Barbasz, A., and M. Oćwieja. 2016. 'Gold nanoparticles and ions – friends or foes? As they are seen by human cells U-937 and HL-60', *Journal of Experimental Nanoscience*, 11: 564-80.

Barreto, A., A. Dias, B. Duarte, E. Pinto, A. Almeida, T. Trindade, A. M. V. M. Soares, K. Hylland, S. Loureiro, and M. Oliveira. 2020. 'Biological effects and

730 bioaccumulation of gold in gilthead seabream (*Sparus aurata*) – Nano versus
731 ionic form', *Science of The Total Environment*, 716: 137026.
732 Barreto, A., L. G. Luis, A. V. Girão, T. Trindade, A. M. V. M. Soares, and M.
733 Oliveira. 2015. 'Behavior of colloidal gold nanoparticles in different ionic strength
734 media', *Journal of Nanoparticle Research*, 17: 1-13.
735 Barreto, A., L. G. Luis, A. M. V. M. Soares, P. Paíga, L. H. M. L. M. Santos, C.
736 Delerue-Matos, K. Hylland, S. Loureiro, and M. Oliveira. 2017. 'Genotoxicity of
737 gemfibrozil in the gilthead seabream (*Sparus aurata*)', *Mutation Research -*
738 *Genetic Toxicology and Environmental Mutagenesis*, 821:36-42.
739 Barreto, A., L. G. Luis, E. Pinto, A. Almeida, P. Paíga, L. H. M. L. M. Santos,
740 C. Delerue-Matos, T. Trindade, A. M. V. M. Soares, K. Hylland, S. Loureiro, and
741 M. Oliveira. 2019a. 'Genotoxicity of gold nanoparticles in the gilthead seabream
742 (*Sparus aurata*) after single exposure and combined with the pharmaceutical
743 gemfibrozil', *Chemosphere*, 220: 11-19.
744 Barreto, A., L. G. Luis, E. Pinto, A. Almeida, P. Paíga, L. H. M. L. M. Santos,
745 C. Delerue-Matos, T. Trindade, A. M. V. M. Soares, K. Hylland, S. Loureiro, and
746 M. Oliveira. 2019b. Effects and bioaccumulation of gold nanoparticles in the
747 gilthead seabream (*Sparus aurata*) – Single and combined exposures with
748 gemfibrozil', *Chemosphere*, 215: 248-260.
749 Barreto, A., L. G. Luis, P. Paíga, L. H. M. L. M. Santos, C. Delerue-Matos, A.
750 M. V. M. Soares, K. Hylland, S. Loureiro, and M. Oliveira. 2018. 'A multibiomarker
751 approach highlights effects induced by the human pharmaceutical gemfibrozil to
752 gilthead seabream Sparus aurata', *Aquatic Toxicology*, 200: 266-274.
753 Best, S. L., and P. J. Sadler. 1996. 'Gold drugs: Mechanism of action and
754 toxicity', *Gold Bulletin*, 29: 87-93.

Bihari, P., M. Vippola, S. Schultes, M. Praetner, A. Khandoga, C. Reichel, C. Coester, T. Tuomi, M. Rehberg, and F. Krombach. 2008. 'Optimized dispersion of nanoparticles for biological *in vitro* and *in vivo* studies', *Particle and Fibre Toxicology*, 5: 14.

Bradford, M. M. 1976. 'A rapid and sensitive method for the quantitation of microgram quantities of protein utilizing the principle of protein-dye binding', *Analytical Biochemistry*, 72: 248-54.

Carlberg, I., and B. Mannervik. 1975. 'Purification and characterization of the flavoenzyme glutathione reductase from rat liver', *Journal of Biological Chemistry*, 250: 5475-80.

Chemello, G., B. Randazzo, M. Zarantoniello, A. P. Fifi, S. Aversa, C. Ballarin, G. Radaelli, M. Magro, and I. Olivotto. 2019. 'Safety assessment of antibiotic administration by magnetic nanoparticles in in vitro zebrafish liver and intestine cultures', *Comparative Biochemistry and Physiology Part C: Toxicology & Pharmacology*, 224: 108559.

Chen, H., A. Dorrigan, S. Saad, D. J. Hare, M. B. Cortie, and S. M. Valenzuela. 2013. *'In vivo* study of spherical gold nanoparticles: inflammatory effects and distribution in mice', *Plos One*, 8: e58208.

Claiborne, A. 1985. 'Catalase activity', *CRC handbook of methods for oxygen radical research*, 1: 283-84.

Collins, A. R. 2004. 'The comet assay for DNA damage and repair', *Molecular Biotechnology*, 26: 249-61.

Connor, E. E., J. Mwamuka, A. Gole, C. J. Murphy, and M. D. Wyatt. 2005. 'Gold nanoparticles are taken up by human cells but do not cause acute cytotoxicity', *Small*, 1: 325-27.

780 Durán, N., C. P. Silveira, M. Durán, and D. S. T. Martinez. 2015. 'Silver
781 nanoparticle protein corona and toxicity: a mini-review', *Journal of*
782 *Nanobiotechnology*, 13: 55.
783 Fang, Y., A. Karnjanapiboonwong, D. A. Chase, J. Wang, A. N. Morse, and T.
784 A. Anderson. 2012. 'Occurrence, fate, and persistence of gemfibrozil in water and
785 soil', *Environmental Toxicology and Chemistry*, 31: 550-55.
786 Farkas, J., P. Christian, J. A. G. Urrea, N. Roos, M. Hassellöv, K. E. Tollefsen,
787 and K. V. Thomas. 2010. 'Effects of silver and gold nanoparticles on rainbow trout
788 (*Oncorhynchus mykiss*) hepatocytes', *Aquatic Toxicology*, 96: 44-52.
789 Filho, D., T. Tribess, C. Gáspari, F. D. Claudio, M. A. Torres, and A. R. M.
790 Magalhães. 2001. 'Seasonal changes in antioxidant defenses of the digestive
791 gland of the brown mussel (*Perna perna*)', *Aquaculture*, 203: 149-58.
792 Fraga, S., H. Faria, M. E. Soares, J. A. Duarte, L. Soares, E. Pereira, C. Costa-
793 Pereira, J. P. Teixeira, M. de L. Bastos, and H. Carmo. 2013. 'Influence of the
794 surface coating on the cytotoxicity, genotoxicity and uptake of gold nanoparticles
795 in human HepG2 cells', *Journal of Applied Toxicology*, 33: 1111-19.
796 Franco, M. E., B. N. Hill, B. W. Brooks, and R. Lavado. 2019. '*Prymnesium*
797 *parvum* differentially triggers sublethal fish antioxidant responses in vitro among
798 salinity and nutrient conditions', *Aquatic Toxicology*, 213: 105214.
799 Frasco, M. F., and L. Guilhermino. 2002. 'Effects of dimethoate and beta-
800 naphthoflavone on selected biomarkers of *Poecilia reticulata'*, *Fish Physiology*
801 *and Biochemistry*, 26: 149-56.
802 García-Negrete, C. A., J. Blasco, M. Volland, T. C. Rojas, M. Hampel, A.
803 Lapresta-Fernández, M. C. Jiménez de Haro, M. Soto, and A. Fernández. 2013.
804 'Behaviour of Au-citrate nanoparticles in seawater and accumulation in bivalves

at environmentally relevant concentrations', *Environmental Pollution*, 174: 134-41.

Goodman, C. M., C. D. McCusker, T. Yilmaz, and V. M. Rotello. 2004. 'Toxicity of gold nanoparticles functionalized with cationic and anionic side chains', *Bioconjugate Chemistry*, 15: 897-900.

Habig, W. H., M. J. Pabst, and W. B. Jakoby. 1974. 'Glutathione S-Transferases. The first enzymatic step in mercapturic acid formation', *Journal of Biological Chemistry*, 249: 7130-39.

Iswarya, V., J. Manivannan, A. De, S. Paul, R. Roy, J. B. Johnson, R. Kundu, N. Chandrasekaran, A. Mukherjee, and A. Mukherjee. 2016. 'Surface capping and size-dependent toxicity of gold nanoparticles on different trophic levels', *Environmental Science and Pollution Research*, 23: 4844-58.

Khan, M. S., G. D. Vishakante, and H. Siddaramaiah. 2013. 'Gold nanoparticles: A paradigm shift in biomedical applications', *Advances in Colloid and Interface Science*, 199-200: 44-58.

Kunjiappan, S., C. Bhattacharjee, and R. Chowdhury. 2015. 'Hepatoprotective and antioxidant effects of *Azolla microphylla* based gold nanoparticles against acetaminophen induced toxicity in a fresh water common carp fish (*Cyprinus carpio* L.)', *Nanomedicine Journal*, 2: 88-110.

Lekeufack, D. Djoumessi, A. Brioude, A. Mouti, J. G. Alauzun, P. Stadelmann, A. W. Coleman, and P. Miele. 2010. 'Core-shell Au@(TiO_2, SiO_2) nanoparticles with tunable morphology', *Chemical Communications*, 46: 4544-46.

Li, J. J., D. Hartono, C.-N. Ong, B.-H. Bay, and L.-Y. L. Yung. 2010. 'Autophagy and oxidative stress associated with gold nanoparticles', *Biomaterials*, 31: 5996-6003.

Lima, I., S. M. Moreira, J. R.-V. Osten, A. M. V. M. Soares, and L. Guilhermino. 2007. 'Biochemical responses of the marine mussel *Mytilus galloprovincialis* to petrochemical environmental contamination along the North-western coast of Portugal', *Chemosphere*, 66: 1230-42.

Luis, L. G., A. Barreto, T. Trindade, A. M. V. M. Soares, and M. Oliveira. 2016. 'Effects of emerging contaminants on neurotransmission and biotransformation in marine organisms – An *in vitro* approach', *Marine Pollution Bulletin*, 106: 236-44.

Mahl, D., J. Diendorf, S. Ristig, C. Greulich, Z.-A. Li, M. Farle, M. Köller, and M. Epple. 2012. 'Silver, gold, and alloyed silver–gold nanoparticles: characterization and comparative cell-biologic action', *Journal of Nanoparticle Research*, 14: 1-13.

Mahl, D., C. Greulich, W. Meyer-Zaika, M. Koller, and M. Epple. 2010. 'Gold nanoparticles: dispersibility in biological media and cell-biological effect', *Journal of Materials Chemistry*, 20: 6176-81.

NIST. 2010. 'NCL method PCC-8, determination of gold in rat tissue with inductively coupled plasma mass spectrometry'.

Ohkawa, Hiroshi, Nobuko Ohishi, and Kunio Yagi. 1979. 'Assay for lipid peroxides in animal tissues by thiobarbituric acid reaction', *Analytical Biochemistry*, 95: 351-58.

Oliveira, M., M. Santos, C. Gravato, and M. Pacheco. 2003. 'Chromium effects on *Anguilla anguilla* liver organ culture', *Fresenius Environmental Bulletin*, 12: 349-52.

Mateo, D., P. Morales, A. Ávalos, and A. Haza 2014. 'Oxidative stress contributes to gold nanoparticle-induced cytotoxicity in human tumor cells'. 2014. *Toxicology Mechanisms and Methods*, 24: 161-72.

Paino, L. M. Martinez, V. S. Marangoni, R. de C. S. de Oliveira, L. M. G. Antunes, and V. Zucolotto. 2012. 'Cyto and genotoxicity of gold nanoparticles in human hepatocellular carcinoma and peripheral blood mononuclear cells', *Toxicology Letters*, 215: 119-25.

Pan, Y., A. Leifert, D. Ruau, S. Neuss, J. Bornemann, G. Schmid, W. Brandau, U. Simon, and W. Jahnen-Dechent. 2009. 'Gold nanoparticles of diameter 1.4 nm trigger necrosis by oxidative stress and mitochondrial damage', *Small*, 5: 2067-76.

Panessa-Warren, B. J., J. B. Warren, M. M. Maye, D. V. D. Lelie, O. Gang, S. Wong, B. Ghebrehiwet, G. Tortora, and J. Misewich. 2008. 'Human epithelial cell processing of carbon and gold nanoparticles', *International Journal of Nanotechnology*, 5: 55-91.

Peng, C., W. Zhang, H. Gao, Y. Li, X. Tong, K. Li, X. Zhu, Y. Wang, and Y. Chen. 2017. 'Behavior and Potential Impacts of Metal-Based Engineered Nanoparticles in Aquatic Environments', *Nanomaterials*, 7: 21.

Schulz, M., L. Ma-Hock, S. Brill, V. Strauss, S. Treumann, S. Gröters, B. van Ravenzwaay, and R. Landsiedel. 2012. 'Investigation on the genotoxicity of different sizes of gold nanoparticles administered to the lungs of rats', *Mutation Research/Genetic Toxicology and Environmental Mutagenesis*, 745: 51-57.

Shiba, F. 2013. 'Size control of monodisperse Au nanoparticles synthesized via a citrate reduction process associated with a pH-shifting procedure', *CrystEngComm*, 15: 8412-15.

878 Shukla, R., V. Bansal, M. Chaudhary, A. Basu, R. R. Bhonde, and M. Sastry.
879 2005. 'Biocompatibility of gold nanoparticles and their endocytotic fate inside the
880 cellular compartment: a microscopic overview', *Langmuir*, 21: 10644-54.
881 Simpson, C. A., K. J. Salleng, D. E. Cliffel, and D. L. Feldheim. 2013. '*In vivo*
882 toxicity, biodistribution, and clearance of glutathione-coated gold nanoparticles',
883 *Nanomedicine: Nanotechnology, Biology and Medicine*, 9: 257-63.
884 Singh, N. P., M. T. McCoy, R. R. Tice, and E. L. Schneider. 1988. 'A simple
885 technique for quantitation of low levels of DNA damage in individual cells',
886 *Experimental Cell Research*, 175: 184-91.
887 Soldatow, V. Y. , E. L. LeCluyse, L. G. Griffith, and I. Rusyn. 2013. *'In vitro*
888 models for liver toxicity testing', *Toxicology Research*, 2: 23-39.
889 Sonavane, G., K. Tomoda, A. Sano, H. Ohshima, H. Terada, and K. Makino.
890 2008. *'In vitro* permeation of gold nanoparticles through rat skin and rat intestine:
891 effect of particle size', *Colloids and Surfaces B: Biointerfaces*, 65: 1-10.
892 Tiede, K., M. Hassellöv, E. Breitbarth, Q. Chaudhry, and A. B. A. Boxall. 2009.
893 'Considerations for environmental fate and ecotoxicity testing to support
894 environmental risk assessments for engineered nanoparticles', *Journal of*
895 *Chromatography A*, 1216: 503-09.
896 Tkachenko, A. G., H. Xie, Y. Liu, D. Coleman, J. Ryan, W. R. Glomm, M. K.
897 Shipton, S. Franzen, and D. L. Feldheim. 2004. 'Cellular trajectories of peptide-
898 modified gold particle complexes: comparison of nuclear localization signals and
899 peptide transduction domains', *Bioconjugate Chemistry*, 15: 482-90.
900 Zeilinger, K., N. Freyer, G. Damm, D. Seehofer, and F. Knöspel. 2016. 'Cell
901 sources for *in vitro* human liver cell culture models', *Experimental Biology and*
902 *Medicine*, 241: 1684-98.

Zeng, S., M. Cai, H. Liang, and J. Hao. 2012. 'Size-dependent colorimetric visual detection of melamine in milk at 10 ppb level by citrate-stabilized Au nanoparticles', *Analytical Methods*, 4: 2499-505.

Zurita, J. L., G. Repetto, Á. Jos, M. Salguero, M. López-Artíguez, and A. M. Cameán. 2007. 'Toxicological effects of the lipid regulator gemfibrozil in four aquatic systems', *Aquatic Toxicology*, 81: 106-15.